

# A Neural-Network Approach for Semiconductor Wafer Post-Sawing Inspection

Chao-Ton Su, Taho Yang, and Chir-Mour Ke

**Abstract**—Semiconductor wafer post-sawing requires full inspection to assure defect-free outgoing dies. A defect problem is usually identified through visual judgment by the aid of a scanning electron microscope. By this means, potential misjudgment may be introduced into the inspection process due to human fatigue. In addition, the full inspection process can incur significant personnel costs. This research proposed a neural-network approach for semiconductor wafer post-sawing inspection. Three types of neural networks: backpropagation, radial basis function network, and learning vector quantization, were proposed and tested. The inspection time by the proposed approach was less than one second per die, which is efficient enough for a practical application purpose. The pros and cons for the proposed methodology in comparison with two other inspection methods, visual inspection and feature extraction inspection, are discussed. Empirical results showed promise for the proposed approach to solve real-world applications. Finally, we proposed a neural-network-based automatic inspection system framework as future research opportunities.

**Index Terms**—Defect, neural network, post-sawing inspection, semiconductor wafer.

## I. INTRODUCTION

THE USE of integrated circuits (ICs) has been rapidly increasing and will continue to increase in the foreseeable future. Therefore, semiconductor manufacturing continues to be in the spotlight of global manufacturing industries [1]. According to SEMI statistics [2], worldwide semiconductor manufacturing equipment sales totaled \$21.9 billion for the first half of 2000, which surpassed the entire 1998 market. Although a semiconductor fabrication process utilizes highly automated and precisely monitored tools in clean-room environment, process variation remains the major challenge in the course of yield enhancement. The sources of variation are from different stages of the manufacturing process. Materials, equipment, operations, etc., can cause the problems. A significant amount of research has aimed at improving the process yield by investigating and developing yield management methodologies at different process stages [3]–[5].

Post-sawing inspection is relatively imprecise inspection step especially compared to others such as laser scanning, wafer acceptance testing, etc., however it requires full inspection to as-

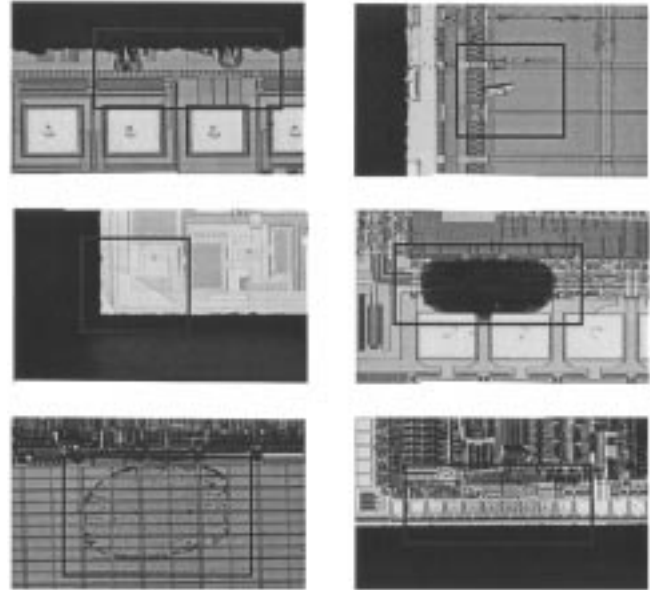


Fig. 1. Commonly seen post-sawing defect types.

sure defect-free outgoing dies. A technician is usually dedicated to this task. Using a scanning electron microscope (SEM), a defect is then identified by the technician's visual judgment. Potential inspection errors may be introduced into the inspection process due to human fatigue. In addition, the full inspection process can incur significant personnel costs.

There are several commonly seen defect types for wafer post-sawing. They are crack, scratch, passivation coverage, ink spot, foreign material pollution, and pad discolor as illustrated in Fig. 1.

Zhang *et al.* [6] developed an automatic post-sawing inspection system using computer vision techniques. The system first extracted boundary features from reference images that were then compared with incoming dies for defect identification by a rule-based algorithm. The use of this approach was limited to boundary defect problems such as chip out and dies crack. The inspection time by this approach was about thirty minutes per wafer. Existing methods for defect identification problems mainly used a feature extraction approach, e.g., Chen and Liu [7] and Sreenivasan *et al.* [8]. The use of these approaches was restricted to learned patterns, e.g., specific defect patterns and to predetermined regions, e.g., die boundary. Furthermore, they are usually time-consuming for in-line implementation. We are not aware of any literature that proposes to solve the post-sawing inspection problem by looking at the whole die area or any that is efficient enough for a practical application.

Manuscript received February 24, 2001; revised January 14, 2002.

C.-T. Su is with the Department of Industrial Engineering and Management, National Chiao Tung University, 1Hsinchu 300, Taiwan, R.O.C. (e-mail: ctsu@cc.nctu.edu.tw).

T. Yang is with the Institute of Manufacturing Engineering, National Cheng Kung University, Tainan 701, Taiwan; R.O.C. (e-mail: tyang@mail.ncku.edu.tw).

C.-M. Ke is with the Lightsonic Optoelectronics Inc., Chunan Miaoli 350, Taiwan; R.O.C. (e-mail: chirmour@loi.com.tw).

Publisher Item Identifier S 0894-6507(02)04457-3.

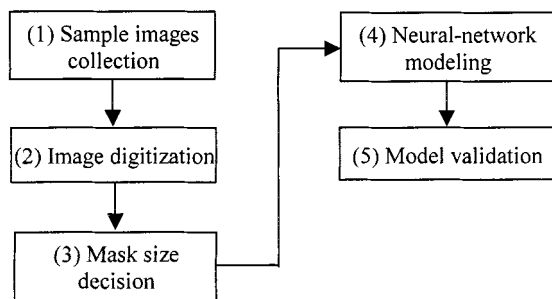


Fig. 2. Proposed approach.

This research proposed a neural-network approach for post-sawing inspection. There are several advantages for using a neural network to solve a complex manufacturing system problem. They are: 1) processing speed through massive parallelism; 2) learning and adapting by means of efficient knowledge acquisition; 3) robustness with respect to fabrication and different failures; and 4) compact processors for space- and power-constrained applications, etc. [9].

For the proposed approach, images were gathered from a set of sample dies by using SEM. These images were then digitized using gray levels, and were used for neural-network training and testing samples. Three neural learning methods were proposed and tested. They are backpropagation (BP), radial basis function (RBF), and learning vector quantization (LVQ) networks. Their respective pros and cons in solving the proposed problem are discussed. Empirical results illustrate the effectiveness and efficiency of the proposed approach.

The remainder of this paper is organized as follows. Section II provides the detailed discussions for the proposed approach. Empirical illustrations are discussed in Section III. Conclusions are then given in Section IV.

## II. PROPOSED APPROACH

There are five major steps for the proposed neural-network approach as shown in Fig. 2.

1) *Sample images collection*: Valid input data are essential in knowledge learning for an artificial intelligence approach. The sample images are collected from both good and defective dies. The defective ones should include the most commonly seen defects for the neural-network training purpose.

2) *Image digitization and 3) mask size decision*: The image digitization converts the brightness of each pixel to a gray level. When one pixel represents one neural-network input node, the number of input nodes becomes intractable in addition to the influences of image noises. To alleviate the network size problem, a proper mask size is defined to represent a neural-network input node. Mask size is a rectangular area comprised of  $N_1 \times N_2$  pixels, where  $N_1$  and  $N_2$  are the number of pixels for rectangular width and length, respectively. The average value of the gray levels of the pixels inside the same mask is used to represent one input node. When both  $N_1$  and  $N_2$  equal one, each pixel represents one node, which represents an extreme case. In general, the larger the mask size is, the fewer the neural-network input nodes will be. Fewer input nodes may reduce model effectiveness. The determination of the number of input nodes is a

tradeoff between training efficiency and model effectiveness. In this research, we incrementally increase the mask size, and then choose the one that provides the best defect inspection results in terms of prediction accuracy as the final mask size setup.

4) *Neural-network modeling and 5) model validation*: The design of an efficient neural-network, post-sawing inspection system is not straightforward. It requires an appropriate choice for the neural paradigm and a fine-tuning of the network topology to find a suitable compromise between performance and computational complexity. Three types of supervised neural networks are applied to the proposed problem and are discussed as follows.

The BP network has input, hidden, and output layers. Usually, there are one to two hidden layers [10]. There are two user-defined parameters: learning rate and momentum, the selections of which have effects on computation efficiency. General rules have been reported by Lippmann [11]. Readers are referred to Pao [12] and Hou *et al.* [13] for more background reviews for the BP network.

The RBF network has the same basic structure as the BP network, except there is only one hidden layer. In addition, there are no connection weights between the input layer and the hidden layer. Its learning process iteratively adjusts the center and shape of the receptive field functions. Learning rate and momentum values are also user inputs. The RBF network features both a simple structure and fast learning. Accordingly, it becomes one of the candidates for the proposed problem. Further information may be found in Jang *et al.* [14].

LVQ is an adaptive data classification method based on training data with desired class information. Although it is a supervised training method, LVQ employs unsupervised data-clustering techniques to process the data set and obtain cluster centers. There are two user-defined parameters: the number of Kohonen nodes for the output layer and the learning rate. Readers can find additional information for the LVQ network in Gupta *et al.* [15].

Model validation uses testing samples to calculate model accuracy. When a validated model is available, it is ready to be launched for the in-line implementation.

## III. EMPIRICAL ILLUSTRATION

### A. Sample Images Collection

For the purpose of an empirical illustration, we collected data from an integrated IC back-end service provider located in Hsinchu, Taiwan. Our study was conducted in one of its production lines, which is dedicated to the inspection of the die size of  $1.71 \times 1.89 \text{ mm}^2$ . An in-line SEM ( $\times 50$ ) was used to extract the die image. In order to collect enough training patterns, we deliberately collected thirty defective dies that contained those commonly seen defect types in addition to ten good dies. The image processing and neural-network training were performed by Ulead PhotoImpact v5.0 and Neural Works Professional II/PLUS v5.3, respectively.

### B. Image Digitization

The SEM took a die image by placing it on the top of a piece of black paper. The procedure for image process started by ad-

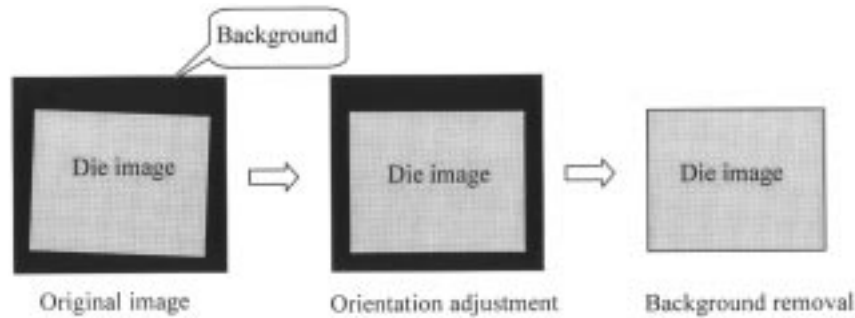


Fig. 3. Image processing.

justing the image's orientation, then its background is removed as shown in Fig. 3. For experimental purpose, orientation adjustment is performed manually while background removal is done by PhotoImpact. Currently, this manual process is time consuming, e.g., tens of seconds to a few minutes. For future in-line implementation, we can automate this process by customized computing codes such as C programming language.

The original images from the single-product production line were 24-bit colored and contained  $293 \times 284$  pixels. When there are more than one product types, e.g., different die sizes, an additional neural-network input node is required to represent product types for model training. For this instance, we need to collect samples from all product types, and then train the model with a product-type input node in addition to the previous network structure. The image was converted to 8-bit gray levels (0–255) by Matlab v5.3 to simplify the neural-network learning complexity. For the convenience of the mask size decision discussed in the following section, a minor border cut was applied to produce a  $288 \times 280$  pixels image. Preliminary studies by observations and by interviews with quality assurance engineers showed that this minor cut would not affect the inspection result, e.g., border crack defect.

### C. Mask Size Decision

The case study used six different mask sizes, which determined their corresponding neural-network input nodes as shown in Table I. The number of input nodes was the division of die size to its mask size. For example, when mask size is  $(32 \times 28)$  pixels, the number of input nodes is:  $(288 \times 280)/(32 \times 28) = 90$ . The resulting mapping address (input node number) is illustrated as Fig. 4.

### D. Neural-Network Modeling and Model Validation

The forty sample dies were randomly separated into two groups: training and testing as shown in Table II.

One hidden layer is usually adopted for modeling training, unless we cannot achieve an acceptable result. Learning iteration, learning rate, momentum and the number of nodes in the hidden layer are the four parameters for neural-network model training. LVQ has no momentum parameters. For the learning iteration decision, we first fixed the momentum and the learning rate at a predetermined level. Then, the model training continued until a stable and acceptable root-mean-square error (RMSE)

TABLE I  
MASK SIZES

Mask size ( $n \times m$ )	Number of input nodes
896 (32×28)	90
672 (24×28)	120
480 (24×20)	168
360 (18×20)	224
320 (16×20)	252
224 (16×14)	360

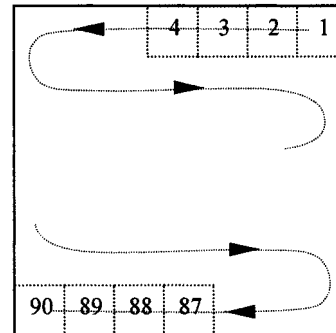


Fig. 4. Mapping address for a die with 90 masks.

TABLE II  
NEURAL-NETWORK DATA GROUPING

Training group		Testing group	
No. of good dies	No. of defective dies	No. of good dies	No. of defective dies
7	23	3	7

was obtained. The RMSE is defined as shown in (1) for measuring the neural-network modeling errors.

$$\text{RMSE} = \frac{1}{s} \sqrt{\sum_{i=1}^s (Y_i - \hat{Y}_i)^2} \quad (1)$$

where  $s$ ,  $Y_i$ , and  $\hat{Y}_i$  are the number of samples, actual response of sample  $i$ , and predicted response of sample  $i$ , respectively.  $Y_i$  is either 0 or 1 to represent a bad or a good die, respectively.  $\hat{Y}_i$  is a real number between 0 and 1 from the neural-network model. The RMSE decreases as the number of iterations increase. Experimental results also showed that the decision of iteration number is not sensitive to momentum and learning rate. Therefore, we chose values from commonly seen rates for the learning rate, momentum, and the number of hidden

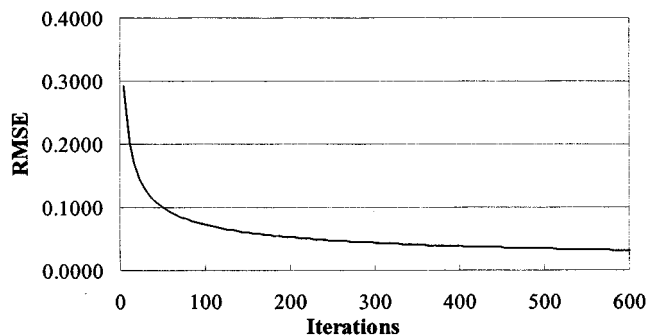


Fig. 5. RMSE versus number of iterations example.

TABLE III  
NEURAL-NETWORK PARAMETERS SETUPS

	Mask size	No. of input nodes	Learning iterations	Learning rate	Momentum
BP	896	90	400	0.8	0.2
	672	120	400	0.8	0.2
	480	168	400	0.8	0.2
	360	224	400	0.8	0.2
	320	252	400	0.8	0.2
RBF	224	360	400	0.8	0.2
	896	90	150	0.4	0.05
	672	120	150	0.4	0.1
	480	168	150	0.4	0.1
	360	224	150	0.4	0.1
LVQ	320	252	150	0.4	0.1
	224	360	150	0.4	0.05
	896	90	100	0.01	N/A
	672	120	100	0.05	N/A
	480	168	100	0.05	N/A
	360	224	100	0.05	N/A
	320	252	100	0.05	N/A
	224	360	100	0.05	N/A

layer nodes of [0.6–0.9], [0.1–0.4], and [10–30], respectively. Through several trial-and-error iterations, we chose 0.8, 0.2, and 20 for learning rate, momentum, and number of hidden nodes, respectively, for iteration number decision.

For example, the relationship between the RMSE and the number of iterations for a BP neural-network model with 90, 0.8, 0.2, and 20, as the values of input nodes, learning rate, momentum, and number of hidden layer nodes, respectively, is shown as Fig. 5. When number of iterations is greater than 400, a stable and low RMSE is obtained. We can then conservatively determine 400 as the terminating iteration number for the BP network training.

Next, we fixed the number of hidden layer nodes at 20 in addition to the terminating iteration decision from the earlier step. For learning rate and momentum parameters, we divided each parameter’s common range into four equal intervals of 0.1. It then resulted in sixteen combinations from different learning rates and momentum levels as: (0.6, 0.1), (0.6, 0.2), (0.6, 0.3), (0.6, 0.4), (0.7, 0.1), (0.7, 0.2), . . . , (0.9, 0.4). The best combination is then chosen as the final parameters value. We repeated the parameters setting procedure for different mask sizes associated with each type of neural network. The results were summarized as shown in Table III.

Finally, we redefine the number of nodes in the hidden layer. Since the model output is to distinguish between a bad and a

TABLE IV  
BACKPROPAGATION NEURAL-NETWORK TRAINING EXAMPLE

No. of nodes in hidden layer	RMSE from training samples	RMSE from testing samples	Accuracy
10	0.0377	0.0419	100.00%
12	0.0342	0.0392	100.00%
14	0.0389	0.0426	100.00%
16	0.0388	0.0411	100.00%
18	0.0398	0.0402	100.00%
20*	0.0356	0.0380	100.00%
22	0.0367	0.0416	100.00%
24	0.0375	0.0411	100.00%
26	0.0398	0.0421	100.00%
28	0.0376	0.0475	100.00%
30	0.0399	0.0455	100.00%

\*Best number of nodes

TABLE V  
NEURAL-NETWORK PARAMETERS SETUP

	Mask size	No. of input nodes	Best No. of nodes in hidden layer	Accuracy
BP	896	90	26	50.00%
	672	120	20	60.00%
	480	168	22	90.00%
	360*	224	20	100.00%
	320	252	26	80.00%
RBF	224	360	12	70.00%
	896	90	10	60.00%
	672	120	18	60.00%
	480	168	14	70.00%
	360*	224	15	90.00%
LVQ	320	252	17	80.00%
	224	360	23	50.00%
	896	90	24	70.00%
	672	120	30	80.00%
	480	168	24	90.00%
	360*	224	18	100.00%
	320	252	24	80.00%
	224	360	18	70.00%

\*Best setup

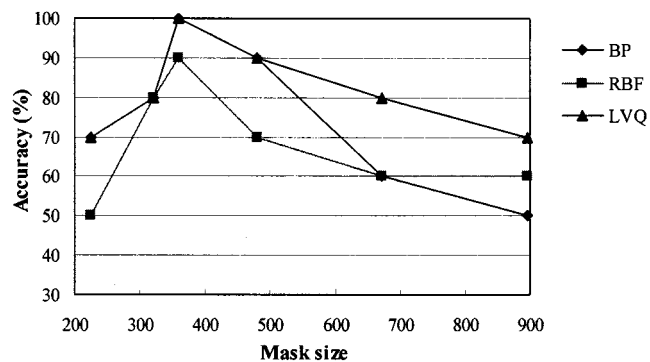


Fig. 6. Accuracy comparisons.

good dies, we conservatively determined two threshold points of 0.2 and 0.8 for a bad and a good dies, respectively. In other words, when the model output value is less (greater) than 0.2 (0.8), the predicted result is a bad (good) die. We then defined prediction accuracy as division of the number of correctly predicted samples to the total number of samples.

For each setup in Table III, we trained a neural network by using different number of nodes in the hidden layer (or Kohonen layer), then the best one was chosen based on the following criteria:

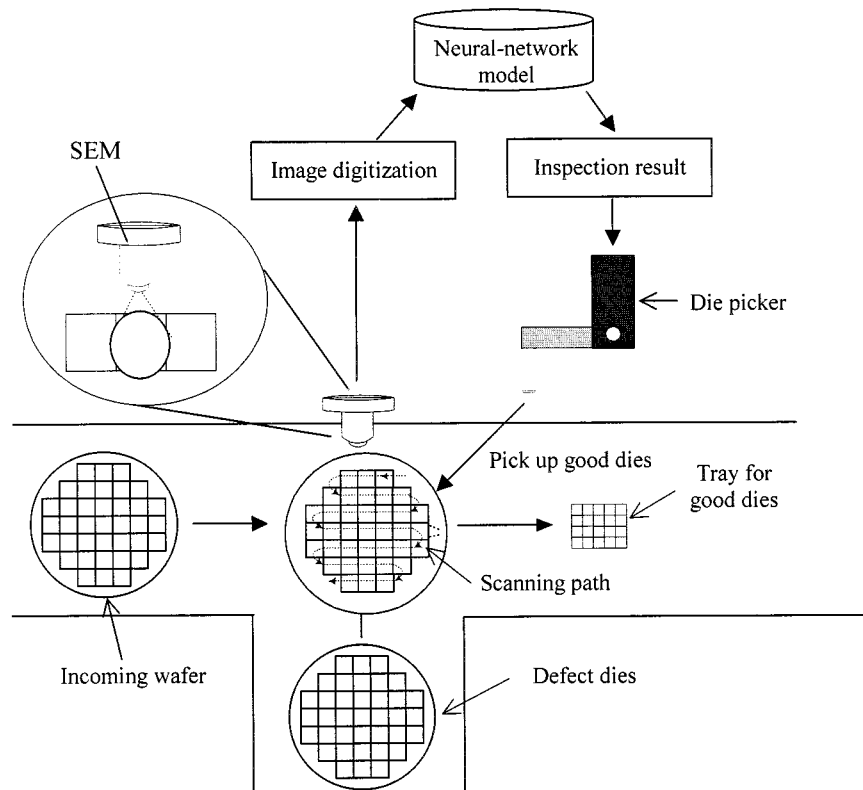


Fig. 7. A neural-network-based automatic inspection system.

TABLE VI  
SUMMARY OF DIFFERENT INSPECTION METHODS

Items	Methods		
	Visual	Neural network	Feature extraction
Inspection area	Whole die area	Whole die area	Partial die area
Accuracy	Medium	High	High
Speed	Slow	Fast	Fast
Stability	Low	High	High
Costs	High	Low	Low
Ease of operation	Difficult	Easy	Easy
System setup lead-time	Short	Long	Long
Flexibility to product complexity	High	Low	High

- 1) the higher the accuracy, the better is the neural-network model;
- 2) minimal RMSE from testing samples;
- 3) minimal RMSE from training samples;
- 4) minimal discrepancy between RMSEs from training and testing samples.

For example, Table IV shows the results using one of the BP network setups (360 for mask size, 224 for input nodes, 400 for learning iterations, 0.8 for learning rate, and 0.2 for momentum) to test the different number of nodes in the hidden layer. The best number of nodes in the hidden layer was 20.

Table V summarized the best number of nodes for each setup and indicated the best setup for each type of neural network. Fig. 6 compared the difference in performance for the three types of networks.

The best setup in terms of accuracy consistently had a mask size of 360 for all three types of networks. Both BP and LVQ

networks reported inspection results with 100% accuracy. The RBF showed inferior results.

The processing time for the proposed approach to report the inspection result for a die was less than one second. If there are 760 dies on a 200-mm wafer, then the inspection time is about thirteen minutes, which is significantly less than thirty minutes required by a computer vision system developed by Zhang *et al.* [6]. In fact, some preliminary experiments showed that it is the die picker (see Fig. 7 for an illustration) that constrains the inspection speed. For example, an automatic die picker takes about 1 second for a pick-and-place cycle.

To evaluate the efficiency and effectiveness of the proposed neural-network system for a practical application, it is compared against two other methodologies, visual and feature extraction methods, with respect to eight key factors: inspection area, accuracy, speed, stability, costs, ease of operation, system setup lead-time, and flexibility. The stability factor is considered to be high when the potential performance deterioration rate is low. The flexibility factor indicates the robustness of the system to

product changes. The other factors are self-explanatory and are not further explained. Table VI shows the pros and cons for the three inspection approaches.

For the case-study company, 100 out of the 200 dedicated inspection operators are devoted to visual die-defect inspection process. The inspection time for each die is usually ranging from 1 to 10 seconds. When the quality of a die can be easily identified, the operator quickly pulls in the next die for inspection and takes about 1 second for this process. On the other hand, when a die seems to have a potential defect, the operator needs more time to perform a more detailed check and may take up to 10 seconds for this process. In addition to the longer inspection time, physical fatigue will add inspection time as well as deterioration in inspection accuracy.

The acquisition costs for an automatic die-pick is about \$85 000. The addition of the neural-network model will cost about \$15 000. Accordingly, the proposed automatic neural-network based inspection system will cost about \$100 000. The feature extraction method has the similar cost. In consideration of the significant manpower for the visual inspection process, an automatic system is potentially efficient and effective in the long run.

The proposed method is easier for model building due to its simpler model training process and less required domain knowledge when it is compared with the feature extraction approach.

In general, the proposed neural-network method embodies superior performance with respect to inspection area, accuracy, speed, stability, costs, and operations. However, it shows inferior setup lead-time performance than visual inspection methodology. In addition, it has the lowest product flexibility. The visual inspection method is more applicable to a high-variety and low-volume manufacturing system, e.g., a research line, due to its negligible setup time. When partial die area inspection is adequate to locate a defect problem, the feature extraction approach may be the best candidate. For a low-variety and high-volume manufacturing system, e.g., a product manufacturing line, the proposed method is the most efficient and effective one.

#### E. System Implementation

When the proposed methodology is introduced into a manufacturing line, it needs to combine with several hardware components including the SEM, conveyor, and die picker to automate the inspection process. Fig. 7 presents a conceptual schema for an automatic inspection system for future implementation.

The conceptual automatic inspection system has a conveyor to transfer a wafer from sawing process to the inspection station. The SEM starts to extract a die image from the upper-right corner of the wafer. The die image is then digitized and processed by the proposed neural-network-based defect inspection system. If the die is normal, then the die picker picks and places it in a tray. Otherwise, the SEM moves forward to extract the next die image along the scanning path. This process continues until all dies are inspected. Then, the wafer with defective dies is moved away. A new inspection cycle commences.

#### IV. CONCLUSION

Post-sawing inspection is a relatively crude inspection step especially compared to others for semiconductor manufacturing processes, however it requires full inspection to assure defect-free outgoing dies. A defect problem is usually identified through visual judgment by the aid of a SEM. Potential inspection errors may be introduced into the inspection process due to human fatigue. In addition, the full inspection process can incur significant personnel costs. This research proposed a neural-network approach for post-sawing inspection. Three types of neural networks were proposed and tested. The inspection time was less than one second per die by the proposed approach. Empirical results showed promise for the proposed approach to solve real-world applications. A conceptual integrated, in-line, neural-network, post-sawing inspection system offers opportunities for future research. Although the proposed neural-network based computing process is not the bottleneck for an inspection cycle, improved computational efficiency will become important to parallel the improved die-picker speed. This is also one of the future research directions.

#### ACKNOWLEDGMENT

The authors would like to thank C. Chen, the Assembly Division Manager of King Yuan Electronics Co., Ltd., for all the supports during the data collection process leading to the results of this research. They are also grateful to two anonymous reviewers for helpful suggestions that improved the presentation of this paper.

#### REFERENCES

- [1] T. Yang, M. Rajasekharan, and B. Peters, "Semiconductor fabrication facilities design using a hybrid search methodology," *Comput. Indust. Eng.*, vol. 36, pp. 565–583, 1999.
- [2] S. T. Myers. (2000) Industry enjoys record year. *Semiconductor Mag.* [Online], vol (10). Available: <http://www.semi.org/web/wmagazine.nsf>
- [3] C. Weber, B. Moslehi, and M. Dutta, "An integrated framework for yield management and defect/fault reduction," *IEEE Trans. Semiconduct. Manufact.*, vol. 8, pp. 110–120, May 1995.
- [4] W. Shindo, E. H. Wang, R. Akella, and A. J. Strojwas, "Effective excursion detection by defect type grouping in in-line inspection and classification," *IEEE Trans. Semiconduct. Manufact.*, vol. 12, pp. 3–9, Feb. 1999.
- [5] C. N. Berglund, "An unified yield model incorporating both defect and parametric defects," *IEEE Transactions on Semiconductor Manufacturing*, vol. 9, pp. 447–454, 1996.
- [6] J.-M. Zhang, R.-M. Lin, and M.-J. J. Wang, "The development of an automatic post-sawing inspection system using computer vision techniques," *Computers in Industry*, vol. 40, pp. 51–60, 1999.
- [7] F.-L. Chen and S.-F. Liu, "A neural-network approach to recognize defect spatial pattern in semiconductor fabrication," *IEEE Trans. Semiconduct. Manufact.*, vol. 13, pp. 366–373, Aug. 2000.
- [8] K. K. Sreenivasan, M. Srinath, and A. Khotanzad, "Automated vision system for inspection of IC pads and bonds," *IEEE Trans. Comp., Hybrids, Manufact. Technol.*, vol. 16, pp. 333–338, May 1993.
- [9] D. Barschdorff and L. Monostori, "Neural networks: Their applications and perspectives in intelligent machining," *Computers in Industry*, vol. 17, pp. 101–119, 1991.
- [10] H. Y. Liao, S. J. Liu, L. H. Chen, and H. R. Tyan, "A bar-code recognition system using backpropagation neural networks," *Eng. Applicat. Artificial Intell.*, vol. 8, pp. 81–90, 1995.
- [11] R. P. Lippmann, "An introduction to computing with neural nets," *IEEE Acoustics, Speech, and Signal Processing Mag.*, vol. 4, pp. 4–22, 1987.
- [12] Y.-H. Pao, *Adaptive Pattern Recognition and Neural Networks*. New York: Addison-Wesley, 1989.

- [13] T.-H. Hou, L. Lin, and P. D. Scott, "A neural network-based automated inspection system with an application to surface mount devices," *Int. J. Production Res.*, vol. 31, no. 5, pp. 1171–1187, 1993.
- [14] J.-S. R. Jang, C.-T. Sun, and E. Mizutani, *Neuro-Fuzzy and Soft Computing*. Upper Saddle River, NJ: Prentice Hall, 1997.
- [15] V. K. Gupta, J. G. Chen, and M. B. Murtaza, "A learning vector quantization neural network model for the classification of industrial construction projects," *Omega*, vol. 25, no. 6, pp. 715–727, 1997.



**Chao-Ton Su** received the Ph.D. degree in industrial engineering from University of Missouri-Columbia, in 1993.

He is a Professor in the Department of Industrial Engineering and Management at National Chiao Tung University, Taiwan. His current research activities include quality engineering, production management and neural networks in industrial applications. He has published articles in *IEEE TRANSACTIONS ON ELECTRONICS PACKAGING MANUFACTURING*, *IIE Transactions*, *European*

*Journal of Operational Research*, *Journal of the Operational Research Society*, *International Journal of Production Research*, *Production Planning and Control*, *International Journal of Production Economics*, *International Journal of Operations and Production Management*, *International Journal of Advanced Manufacturing Technology*, *International Journal of Systems Science*, *Integrated Manufacturing Systems*, *Computers in Industry*, *Computers and Industrial Engineering*, *Journal of Computer Information Systems*, *Journal of Intelligent Manufacturing*, *International Journal of Industrial Engineering*, *Quality Engineering*, *Quality and Reliability Engineering International*, *Reliability Engineering and System Safety*, *International Journal of Quality and Reliability Management*, *International Journal of Quality Science*, *Total Quality Management*, and *Industrial Management and Data Systems*.

Dr. Su obtained the 2000–2001 Outstanding Research Award of the National Science Council of the Republic of China. In 2001, Dr. Su also obtained the Individual Award of the National Quality Awards of the Republic of China.



**Taho Yang** received the B.S. degree in mechanical engineering from National Cheng Kung University, Taiwan, in 1985 and the M.S. degree from the University of Missouri-Columbia in 1992 and the Ph.D. degree in industrial engineering from Texas A&M University, College Station, TX, in 1996.

He is an Associate Professor of Institute of Manufacturing Engineering at the National Cheng Kung University, Taiwan. He was formerly a project manager with Tefen Ltd., an industrial engineering and system analysis company in California. His research

interests are in the design and analysis of manufacturing systems, particularly, in the area of integrated-circuit manufacturing.



**Chir-Mour Ke** received the M.S. degree in industrial engineering and management from National Chiao Tung University, Taiwan, R.O.C., in 2001.

He is an engineer at Lightsonic Optoelectronics Inc., Hsinchu, Taiwan, R.O.C. His current research interests are in operation management and IE methods in TFT industrial applications.